



Numerical modelling of CFS two-storey sheathing-braced building under shaking-table excitations

Alessia Campiche ^{*}, Luigi Fiorino, Raffaele Landolfo

Department of Structures for Engineering and Architecture, University of Naples "Federico II", Naples, Italy



ARTICLE INFO

Article history:

Received 4 November 2019

Received in revised form 15 April 2020

Accepted 16 April 2020

Available online 25 April 2020

Keywords:

Gypsum-sheathed CFS structures

Seismic response

Shake-table tests

Nonlinear building modelling

ABSTRACT

The recent seismic events have highlighted the need of tools for predicting the performance until collapse and hence assisting to minimize the damages and losses. A European project, named ELISSA, has been recently finished, in which the University of Naples Federico II has explored the seismic behaviour of a Cold Formed Steel (CFS) full-scale two-storey building, via shake-table tests on bare structure and complete construction phases of specimen. Starting from experimental results, advanced numerical models have been developed using the OpenSees software, which consider both structural and non-structural elements and their contribution to the response. The comparison between experimental and numerical results showed that the proposed approach can capture the seismic behaviour of tested building, with acceptable prediction of the response in terms of inter-storey drift peaks and time history if structural and non-structural components are explicitly considered. A further task showed that the earthquake sequence effect can affect the results and it should be taken into account for a better numerical prediction.

© 2020 Published by Elsevier Ltd.

1. Introduction

The recent seismic events have highlighted the need to deeply know the dynamic behaviour of structures and the response to earthquake actions, in order to prevent and minimize damages and losses. In the last decades, many studies have been started with the goal of exploring the seismic response of buildings and, among them, shake-table tests have proved to be one of the most effective way to predict the seismic behaviour [1–4]. Focusing mainly on lightweight steel (LWS) constructions, several researches have also been conducted because the use of these structures, especially in seismic areas, is increasing more and more, due to the potential benefits, as low seismic mass and fast erection. The structural elements in the LWS solutions are generally Cold-Formed Steel (CFS) members and the main lateral resistance components are shear walls, which could be either sheathed by flat sheets of steel or by panels made of wood, gypsum or cement-based materials. Although nowadays their capability to exhibit high structural, technological and environmental performances is well known, lack of high-fidelity modelling tools, which engineers could easily use, is evident. In fact, all models developed in the state of the art for whole buildings [5–7] are complex from computational point of view or not very

accurate, also because modelling the response of CFS buildings introduces many potential assumptions. The state of the art of current numerical modelling of CFS structures has been extensively reviewed by the authors elsewhere [8]. The most vital element for simulation of the dynamic response of LWS structures is shear wall. Its nonlinear behaviour is often represented by a so-called "full-panel" model, in which a pair of diagonal truss elements is calibrated on available experimental data, as in the works of Fülöp and Dubina [9], Shamim and Rogers [10], Kechidi and Bourahla [11] and Fiorino et al. [8,12]. A different approach was followed by Martínez-Martínez and Xu [6], in which shear walls were represented by shell elements with equivalent properties.

However, modelling only shear walls is not enough for an accurate prediction of CFS building lateral response and it is evident the need of developing 3D models, which include also other components often neglected. In particular Leng et al. [7,13] presented OpenSees advanced 3D models of a two-storey CFS commercial building sheathed with OSB panels, named as CFS-NEES building. As a part of the Cold-Formed Steel – Network for Earthquake Engineering Simulation (CFS-NEES) research project, the archetype was tested [14–16] in the Summer of 2013 at the NEES shake-table facility at the University of Buffalo. The models developed included both structural and non-structural systems. Structural system was mainly composed of gravity system (stud and track skeleton) and lateral force resisting system (OSB-sheathed shear walls and diaphragms). Non-structural elements mainly consisted of additional OSB and gypsum panels and internal partitions. Different modelling options were used in order to evaluate the contribution of each

* Corresponding author at: Department of Structures for Engineering and Architecture, University of Naples "Federico II", Via Forno Vecchio 36, 80134 Naples, Italy.

E-mail addresses: alessia.campiche@unina.it (A. Campiche), l.fiorino@unina.it (L. Fiorino), landolfo@unina.it (R. Landolfo).

component. In particular, among different modelling options, Authors use also the so-called "sub-panel" approach, which consists in subdividing the sheathed elements into small parts, in order to take into account of the actual framing elements and connections, such as intermediate studs, ledgers, opening headers. In particular, OSB-sheathed shear walls were divided into multiple sub-panels and modelled using nonlinear diagonal truss elements, in which hysteretic behaviour was represented by Pinching4 material; all-steel gravity system elements (studs and tracks) were modelled as beam-column elements; the same approach was used for interior gypsum-sheathed non-structural walls. The main advantage of the sub-panel approach is represented by the possibility to consider the real load path and interaction with shear wall framing. It is suitable to capture the seismic behaviour, especially where openings are present in the building. In order to capture the influence of diaphragm, rigid and semi-rigid diaphragm models were developed. As a result of dynamic identification, the models which included only shear walls and gravity frame had the first period of vibration in short direction equal to 0.33 s and 0.32 s, if rigid diaphragm and semi-rigid diaphragm models were considered respectively, whereas the model which included also gravity exterior walls, interior walls and non-structural gypsum sheathings had a first period of 0.22 s, in case of rigid diaphragm. Experimentally the building with only shear walls sheathed exhibited a first period in the short direction of 0.36 s, while the final complete building showed a value of 0.26 s. As concerned inter-storey drift, the most advanced model well captured peaks in both directions, with a ratio numerical to experimental equal to 1.25 and 1.37 for long and short direction, respectively. Indeed, models seemed to be stiffer than tested building in the elastic range, but less stiff than tested building in the nonlinear range. Moreover, the inclusion of non-structural systems (additional panels and internal partitions) nonetheless, as shown by tests [16,17] and developed models, alters stiffness, damping and response of building, increasing the lateral capacity of the CFS structures, so there is a great need for the development of models which take explicitly into account also the finishing and non-structural systems. Although the presented model can simulate experimental behaviour of the tested archetype accurately, it is still quite computationally complex for some cases, making it a challenge for designers.

Additionally, from the examination of state of the art, it is evident that the goodness of dynamic response modelling is greatly influenced by Rayleigh damping ratio value [10]. For steel structures it is generally fixed to 2%, but for CFS sheathed structures, damping ratio has a big variability (from about 1% to about 8% without non-structural systems), it is higher when non-structural systems are present (from about 3% to about 20%) and it naturally increases with damage, as shown by shake-table tests in Shafer et al. [18], Hoehler et al. [19], Shamim et al. [20,21] and Fiorino et al. [17]. For modelling of CFS building response the choice of damping ratio value is still an open issue. Shamim and

Rogers [10], for shear wall modelling increased gradually damping in order to obtain a reasonable load vs. deformation hysteretic fit and energy dissipation match between the test and the model results and, according to trial procedure results, they suggested a value ranging from 4% to 5%. For whole building modelling performed by the Authors [22], instead, the value chosen was 2%. Bourahla et al. [5] and Leng et al. [7] used a Rayleigh damping of 5% in their building model.

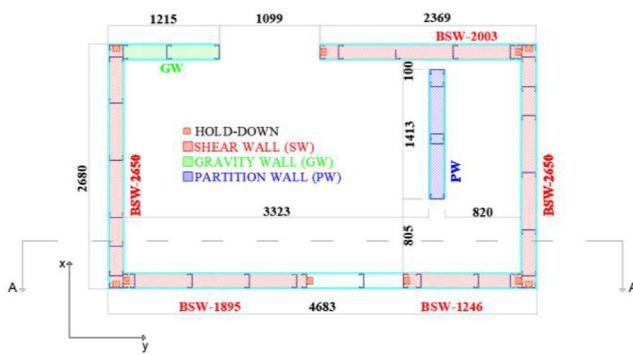
The present work is part of the European project, named as ELISSA (Energy efficient Llightweight-Sustainable-SAfe steel construction), in which an extensively experimental campaign was carried out at Lab of University of Naples "Federico II". In particular, order to evaluate the seismic performance of CFS sheathing-braced buildings, connections test, monotonic and cyclic full-scale wall tests and shake-table tests on a two-storey CFS gypsum sheathing-braced building were performed [17,23] and numerical modelling of single shear walls was developed according to the full-panel approach [8].

This paper provides the details of numerical modelling in OpenSees software of the tested building. The proposed numerical models include all the structural and non-structural elements, remaining quite light from computational point of view. In particular, the paper summarizes the shake-table tests performed on two-storey CFS building sheathed with gypsum panels and presents computationally efficient nonlinear building models developed in OpenSees, which explore the importance of modelling each different component on results. It is organized as follow: Section 2 summarizes tested mock-up properties and shake-table tests; Sections 3 explores the modelling of the mock-up, starting from shear wall models and calibration to 3D building models; Section 4 compares the numerical and the experimental results; Section 5 discusses the obtained results and main parameters affecting them; in Section 6 conclusions and further developments are presented.

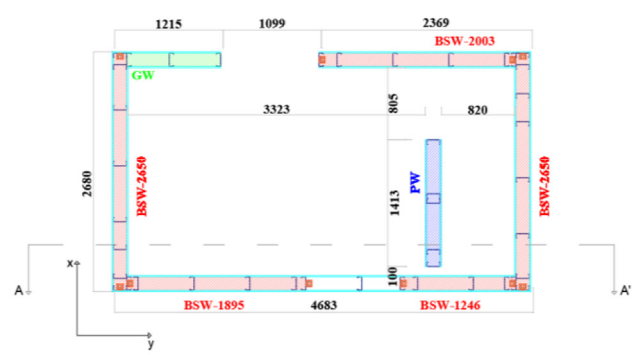
2. Mock-up description and shake-table testing

The ELISSA mock-up was a full-scale two-storey building designed for gravity loads as an "all-steel" solution and for seismic loads as a sheathing-braced solution, in which the seismic resistant elements are made of CFS stud shear walls laterally braced by gypsum panels. The dimensions of the mock-up were about 2.5×4.5 m in plan, with an inter-storey height of about 2.3 m and a total height of about 5.4 m. The mock-up was designed in accordance with current European building codes [24,25] and technical approvals [26]. More details about the research project are available in Landolfo et al. [23].

The mock-up was built in two different stages: in the first phase, named as bare structure (Configuration B), the mock-up was mainly composed of structural components of walls, floors and roof; in the second configuration, named as complete construction (Configuration C), all non-structural components (internal counter walls for gravity and



a) First floor plan



b) Second floor plan

Fig. 1. Plans of mock-up in Configuration B.

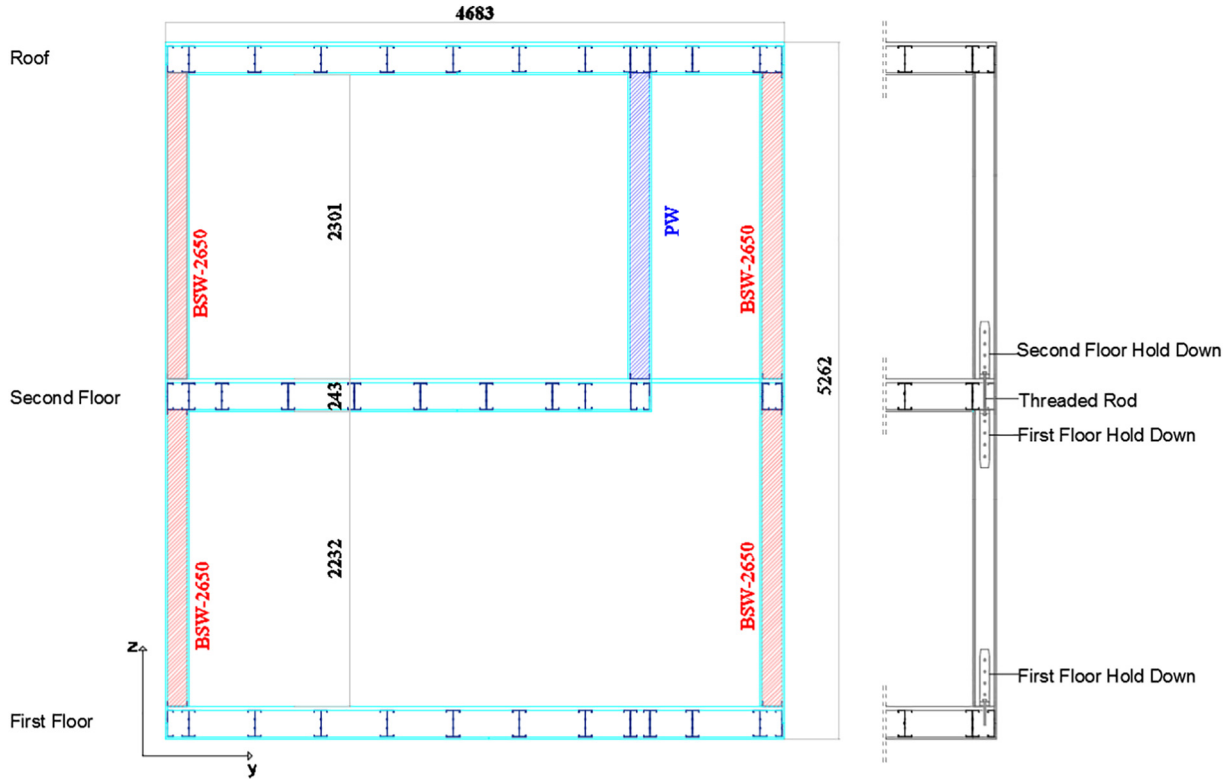


Fig. 2. Vertical section AA' of mock-up.

shear walls and finishing parts for floor and roof) were added to the bare structure. Fig. 1 shows plan views of the mock-up, whereas a vertical section is shown in Fig. 2. Fig. 3 shows main constructional details of structural and non-structural components, i.e. walls, floors and roof. In particular, Figs. 1 and 2 show the mock-up in Configuration B, whereas the differences between Configurations B and C can be evaluated by comparing the constructional details given in Fig. 3.

The mock-up in Configuration B consisted mainly of shear walls and gravity walls without finishing parts, internal partition walls, floors and roof. Shear, gravity and partition walls were built with $147 \times 50 \times 1.5$ mm C studs (steel grade S320GD + Z) with a spacing of about 600 mm on the centre connected at their end with 150×40

$\times 1.5$ mm U wall tracks. Walls were sheathed with 15 mm thick impact resistant gypsum board panels on both sides. Connections between studs and wall tracks were made by self-drilling screws, whereas sheathing panels were connected to steel frame by ballistic nails. The main difference between shear and gravity walls is the presence of hold-down in shear walls. In fact, in order to withstand the axial force due to overturning phenomena, ad hoc designed hold-down devices were placed at the ends of shear wall segments. Internal partition walls, instead, were not designed to carry gravity loads. Floors and roof were made of back-to-back lipped C 197 $\times 50 \times 10 \times 2.0$ mm joists with a spacing of about 500 mm on the centre connected at their end with $200 \times 40 \times 1.5$ mm U floor tracks,

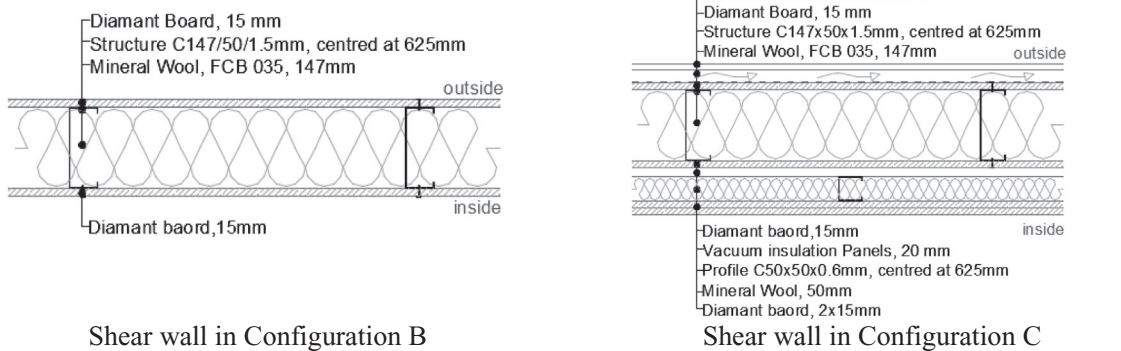


Fig. 3. Main constructional details of structural and non-structural components.

sheathed on the top side with 28 mm thick high-density gypsum fibre board panels. Connections between joists and floor tracks were made by self-drilling screws. Bottom sides of second floor and roof were sheathed with 15 mm thick impact resistant gypsum board panels connected to steel frames.

The mock-up in Configuration C was completed with non-structural elements, which mainly consisted of internal counter walls and finishing parts of shear walls, gravity walls, and finishing parts of floors and roof. In particular, internal counter walls of shear and gravity walls were made of $50 \times 50 \times 0.6$ C non-structural studs spaced at about 600 mm on the centre, connected at their end with $50 \times 40 \times 0.6$ U wall tracks and sheathed only on the internal side with a double layer of 15 mm thick impact resistant gypsum board panels. Internal counter walls were completed with 20 mm thick vacuum insulated panel and 50 mm thick insulation mineral wool. External faces of shear and gravity walls were completed with a ventilated façade. Top sides of first and second floors were sheathed with additional gypsum fibre board panels, whereas bottom sides of second floor and roof were completed with a ceiling.

The seismic weight of the bare structure was evaluated to be approximately 24 kN for the second floor and 14 kN for the roof, while for the complete construction they were approximately 50 kN and 26 kN, respectively. Mock-up pictures in both Configurations and a schematic 3D drawing, in which some structural components are visible, are presented in Fig. 4. Further details about mock-up are available in Fiorino et al. [17].

Two shake-table test typologies were performed: random tests (RND) to evaluate the dynamic properties, such as fundamental period of vibration and damping ratio, and earthquake tests (EA), for the evaluation of the seismic response of the building. For random tests white noise signals (acceleration-controlled flat random noise with a frequency band of 0.5–50 Hz.) were used, while for earthquake tests the selected natural ground motion record was the 2009 L'Aquila earthquake, scaled by factors from 5 to 150%. The used ground motion record is from the AQV Station (Est-West component), located on alluvial soil in the middle of Aterno valley (Soil type B according to soil classification given in EN1998 – Part 1 [24]) at a distance of 4.9 km from epicentre. The original ground motion had a PGA of 6.44 m/s^2 (0.66 g). RND tests were performed on both Configurations B and C, while EA tests were carried out only on Configuration C. It is important to notice that all inputs were applied in the X direction (see Fig. 1), because it represented the worst loading condition for the mock-up. The test program is summarized in Table 1. Further details about shake-table tests are available in Fiorino et al. [17].

3. Development of detailed ELISSA mock-up model

Past modelling [5,6] of seismic response of CFS buildings introduced many simplifications, missing the real behaviour, or it was much complex from computational point of view [7], becoming not useful for designers. In order to overcome this, high-fidelity models of mock-up were developed in OpenSees [27] environment for each phase with the aim to predict accurately the nonlinear dynamic behaviour of the building under seismic excitations and saving computational cost. In fact, although advanced and detailed models are very useful in research applications, simpler models could be a precious goal for some applications in real field scenario. In the following Sections modelling of the mock-up in Configurations B and C is presented, starting from modelling of main structural and non-structural systems. In detail, modelling options of shear walls in Configurations B and C, and other components, i.e. gravity walls, partition walls, floors and internal counter walls, are explored.

3.1. Shear walls

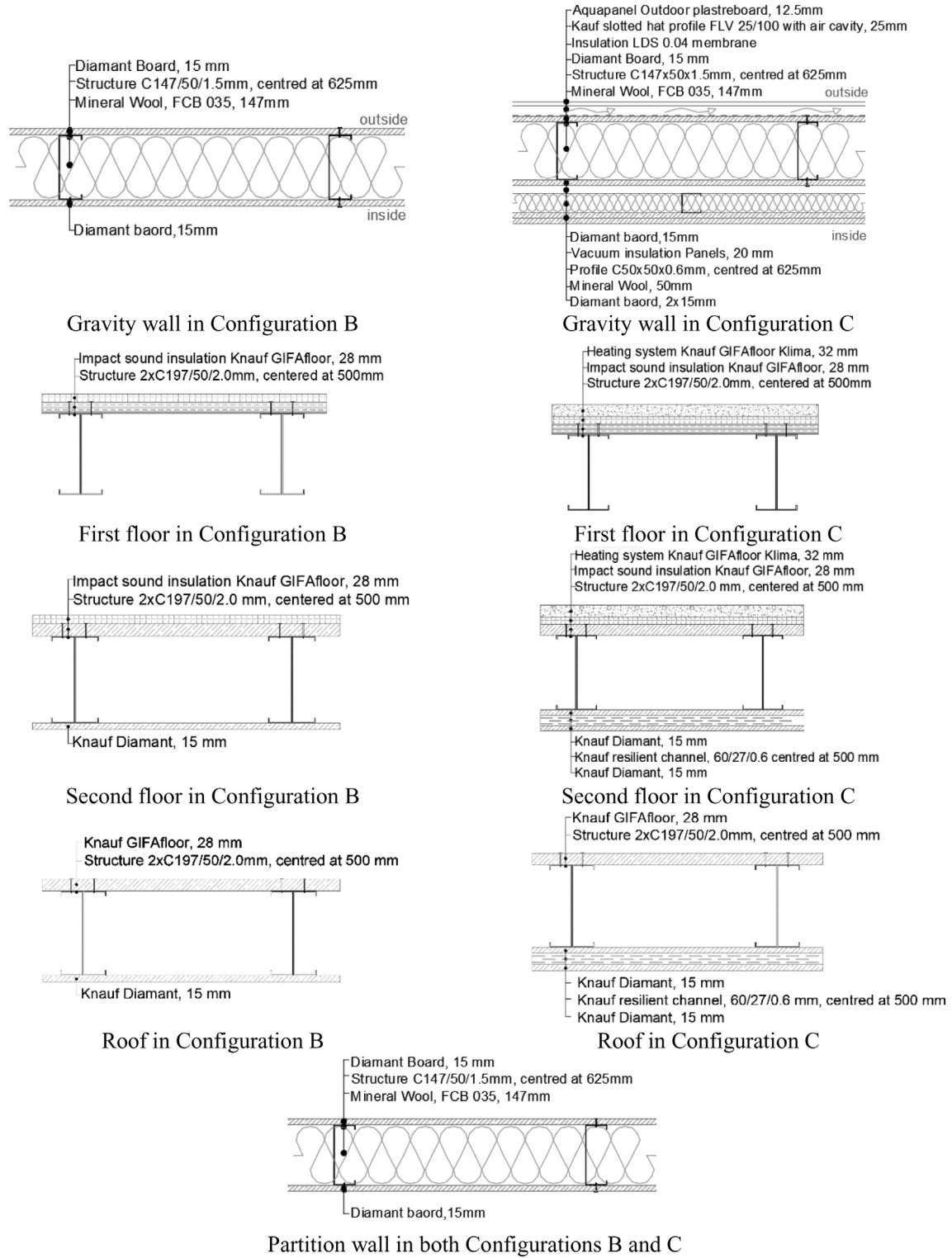
Necessary to the seismic response assessment of a CFS sheathed-panel structure is the shear wall modelling, because its behaviour affects most the lateral response of the whole building. For the ELISSA mock-up modelling eight different shear walls were identified considering the two construction phases, as summarized in Table 2

Two wall specimens representative of the shear wall B-2650 (shear wall in X direction in Configuration B) were also tested under monotonic and quasi static cyclic loading and a single wall specimen C-2650 (shear wall in X direction in Configuration C) were a shear wall representative of the shear wall C-2650 (shear wall in X direction in Configuration C) was tested under quasi static cyclic loading [28].

The shear walls were modelled according to the full-panel approach by a pair of diagonal trusses elements with a *Pinching4* [29] material, calibrated based on quasi static cyclic test response of the walls [28]. Since the mock-up does not present openings in X direction (the direction of the application of seismic load), full-panel approach was preferred to sub-panel approach, employed by Leng et al. [7], saving computational cost. Further discussion about this modelling choice is explained in Paragraph 3.3.

Fig. 7a shows a schematic drawing of the model representative of a shear wall belonging to the first level of the mock-up. *Pinching4* material is a material model, used to idealize a response of uniaxial truss member. It represents a pinched load-deformation response, through 16 parameters defining the 4-point multi-linear law (backbone curve), and it can exhibit degradation under cyclic loading, through 23 parameters defining unloading and reloading stiffness degradation and strength degradation.

In order to define the best-fit *Pinching4* material for the ELISSA shear walls, the force-displacement curves assigned to diagonals were individuated first, which represent the lateral behaviour of the walls, then the cyclic parameters were necessarily calibrated, which regulate the hysteretic behaviour of the walls. Considering shear walls B-2650 and C-2650, the parameters for the *Pinching4* material was defined based on available quasi-static cyclic shear wall tests. In particular, the average envelope curves between the negative and positive branches obtained from experimental cyclic shear wall tests [28] were converted in backbone curves to be implemented in OpenSees. Net global experimental behaviour, excluding the deformability of the hold-downs, was used to calibrate the numerical backbone curve. First point (1) of the numerical backbone curve was placed on the experimental envelope curve at the 20% of the peak strength (F_{\max}), in order to allow the models to capture nonlinear behaviour of walls from beginning and to dissipate energy in the initial cycles. The force at second point (2) of the numerical backbone curve was positioned at 80% or 70% of F_{\max} , for wall B-2650 or C-2650, respectively, whereas the corresponding displacement was chosen with an energy balance, so that the area under the numerical backbone curve until peak was equal to that of the experimental envelope curve. Third point (3) of the numerical backbone curve was the peak point of the experimental envelope curve. The displacement at fourth point (4) of numerical backbone curve was set equal to a drift angle corresponding to a peak strength degradation equal to about 50% in the experimental envelope curve (drift angle of 3.5% and 2.5% for shear wall in Configuration B and C, respectively), whereas the corresponding force was selected with an energy balance, so that the area under the numerical backbone curve between points (3) and (4) was equal to that of the experimental envelope curve. The model was not restricted from going to drifts past the last point, but it never achieved such a big value. Therefore, the choice of the ultimate drift did not matter for this specific model. The values adopted for numerical backbones of B-2650 and C-2650 models are summarized in Table 3. Further details are described in Fiorino et al. [8].

**Fig. 3 (continued).**

In the case of shear wall models for which no experimental data were available, i.e. models of shear walls B-1246, B-1895, B-2003 and C-1246, C-1895, C-2003, the same properties per unit wall length of walls B-2650 and C-2650 were adopted, respectively. In this way a

scale factor equal to L/L_{2650} was used, where L represents the length of the generic shear wall and $L_{2650} = 2650$ mm. Fig. 5 shows the comparison between experimental and numerical backbones for the shear walls B-2650 and C-2650.

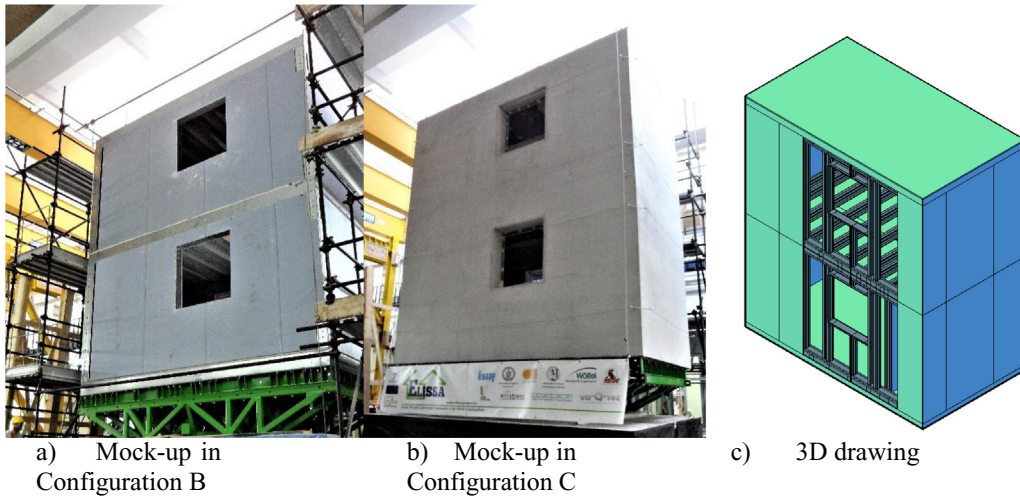


Fig. 4. Mock-up pictures and 3D drawing.

Table 1
Complete test program.

Test name	Input	Level	Stage of construction
RND_1_01, 1_02, 1_03, 1_04, 1_05	White noise	0.05 g, 0.10 g, 0.07 g, 0.07 g (PGA)	B
RND_2_01, 2_02, 2_03	White noise	0.05 g, 0.07 g, 0.10 g (PGA)	C
EA_2_01, 2_02, 2_03, 2_04, 2_05, 2_06, 2_07, 2_08	Earthquake	5%, 10%, 15%, 20%, 25%, 30%, 40%, 50% AQV	C
RND_3_01	White noise	0.10 g (PGA)	C
EA_3_01, 3_02, 3_03, 3_04, 3_05, 3_06, 3_07	Earthquake	20%, 40%, 50%, 60%, 75%, 90%, 100% AQV	C
RND_3_03	White noise	0.10 g (PGA)	C
EA_3_08	Earthquake	50% AQV	C
EA_4_01, 4_02, 4_03, 4_04	Earthquake	50%, 100%, 120%, 100% AQV	C
RND_4_01	White noise	0.10 g (PGA)	C
EA_4_05	Earthquake	100% AQV	C
RND_4_03	White noise	0.10 g (PGA)	C
EA_4_06	Earthquake	50% AQV	C
RND_4_07, 4_09	White noise	0.10 g, 0.10 g (PGA)	C
EA_4_10	Earthquake	50% AQV	C
RND_4_11	White noise	0.10 g (PGA)	C
EA_4_13, 4_14, 4_15, 4_16, 4_17	Earthquake	50%, 75%, 100%, 125%, 150% AQV	C
RND_4_12	White noise	0.10 g (PGA)	C

Table 2
Shear wall model configurations.

Label ^a	Direction	Geometry ^b (H × L)
B – 2650	X	2245 × 2650
B-1246	Y	2245 × 1246
B-1895	Y	2245 × 1895
B – 2003	Y	2245 × 2003
C-2650	X	2245 × 2650
C-1246	Y	2245 × 1246
C-1895	Y	2245 × 1895
C-2003	Y	2245 × 2003

^a B: wall in Configuration B; C: wall in Configuration C.

^b H: wall height; L: wall length.

In order to transform wall behaviour into diagonal behaviour the following expressions (Eqn 1, Eqn 2, Eqn 3, Eqn 4) were used:

$$f = \frac{F}{2 \cos\theta} \quad (1)$$

$$d = \Delta \cos\theta \quad (2)$$

$$\delta = \frac{d}{\sqrt{W^2 + H^2}} \quad (3)$$

Table 3
Numerical backbone values for B-2650 and C-2650 models.

	POINT	F/L[kN/mm]	Drift angle [-]
B-2650	0	0.0000	0.0000
	1	0.0020	0.0002
	2	0.0099	0.0044
	3	0.0124	0.0102
C-2650	4	0.0050	0.0345
	0	0.0000	0.0000
	1	0.0013	0.0001
	2	0.0144	0.0047
	3	0.0180	0.0113
	4	0.0022	0.0256

$$\cos\theta = \frac{1}{\sqrt{1 + \left(\frac{H}{W}\right)^2}} \quad (4)$$

where, F is the force applied during the test on wall top, Δ is the top wall displacement recorded during the test, f is an equivalent stress in a strap of unit area, δ is the axial deformation in the strap, l is the length of the strap and θ is the angle of the diagonal strap respect to bottom track. The shear wall models were subjected to the same loading protocol used in

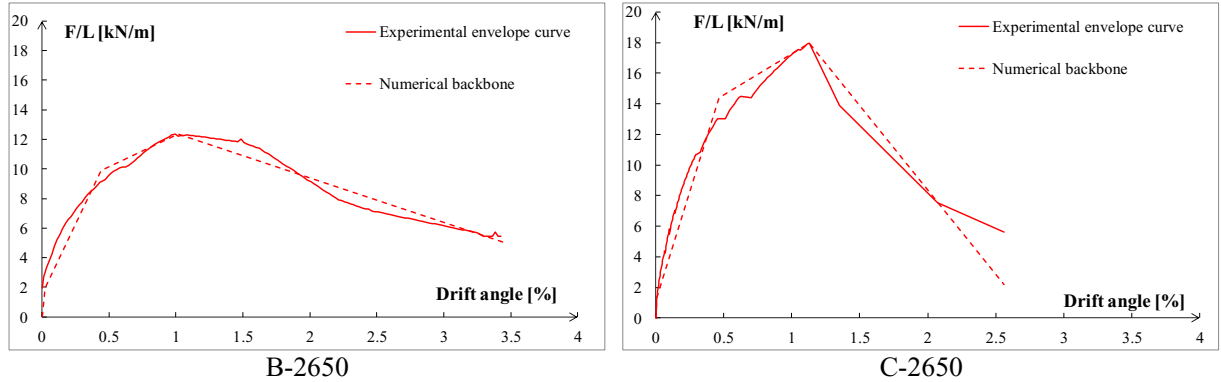


Fig. 5. Comparison between experimental and numerical envelope curves.

the cyclic tests (CUREE protocol [30]). The cyclic parameters involved in *Pinching4* model were chosen with a hit and trial method. A parametrical analysis was conducted to better match the cyclic behaviour of the walls through a quantitative comparison based on the energy dissipation per single cycle (Eqn 5) and cumulative cyclic energy (Eqn 6).

$$\Delta_{E,i} = \frac{E_{n,i} - E_{e,i}}{E_{e,i}} \times 100, [i \leq n] \quad (5)$$

$$\Delta_{CE,j} = \frac{CE_{n,j} - CE_{e,j}}{CE_{e,j}} \times 100 \quad (6)$$

$$CE_{e,j} = \sum_{i=1}^j E_{e,i}, [i, j \leq n] \quad (7)$$

$$CE_{n,j} = \sum_{i=1}^j E_{n,i}, [i, j \leq n] \quad (8)$$

where: $\Delta_{E,i}$ is the difference of the energy dissipation for i^{th} cycle of loading protocol between numerical and experimental results expressed as percentage; $\Delta_{CE,j}$ is the difference of the cumulative energy for the j^{th} cycle of loading protocol between numerical and experimental results expressed as percentage; $CE_{n,j}$ (Eqn 8) and $CE_{e,j}$ (Eqn 7) represent respectively the cumulative energy dissipated for j^{th} cycle of the loading protocol obtained accounting for numerical and experimental results and are evaluated according to Eqs. 7 and 8; $E_{n,i}$ and $E_{e,i}$ represent respectively the energy dissipated in i^{th} cycle of numerical and experimental results; n is the last cycle of the loading protocol (CUREE protocol [30]). The cyclic parameters used in the definition of *Pinching4* material for both models are given in the Table 4. More details are available in Fiorino et al. [8].

The average of the absolute values of $\Delta_{E,i}$ was about 34% and 26% for the shear walls B-2650 and C-2650, respectively, whereas the error $\Delta_{CE,n}$ between numerical and experimental cumulative energy was about 4% and 1%. The value of $\Delta_{CE,n}$ was evaluated at the 43rd cycle of loading protocol for the shear wall B-2650 and at the 40th cycle of loading protocol for the shear wall C-2650. Such small errors indicate that the models well catch the cyclic behaviours of the shear walls. The comparison between experimental and numerical cyclic response for the shear walls B-2650 and C-2650 in term of response curve and dissipated energy is shown in Fig. 6.

ZeroLength elements were used to model the hold-downs present at the ends of shear walls. OpenSees *uniaxialMaterial MinMax* was used in conjunction with *uniaxialMaterial ElasticMultiLinear* to explicitly model the different behaviour in tension and compression and the tensile failure of hold-downs. In particular, based on experimental results [28], the

tensile rupture strain of *uniaxialMaterial MinMax* was set equal to 2.7 (corresponding to a nominal tensile resistance of anchors of 100 kN), whereas for the *uniaxialMaterial ElasticMultiLinear* the tension stiffness of material was set equal to $K_{hd} = 37$ kN/mm and a very high stiffness was used in compression (10^6 kN/mm).

The tracks were modelled by infinite rigid truss elements, whereas a preliminary study was devoted to select the more effective element to be used for the chord studs of the shear walls. In particular, models developed with the chord studs idealized as truss elements and beam column elements were compared. Because the type of element used to model numerical chord studs did not affect the numerical results, the truss element was selected due to its greater computationally efficiency. Therefore, the chord studs were modelled as truss elements with the *uniaxialMaterial Elastic* having the same properties of the profiles used in the mock-up (147 × 50 × 1.5 mm C back-to-back sections). Similar to hold downs, *uniaxialMaterial MinMax* was also used for chord studs to explicitly model buckling mechanisms and tensile rupture, by defining a maximum compressive strain of 6.19×10^{-4} (corresponding to a buckling resistance of 125 kN) and the maximum tensile strain of 1.67×10^{-3} (corresponding to a tensile resistance of 142 kN).

For models in which the intermediate studs were included (Fig. 6b), they were modelled as truss elements with physical and mechanical properties representative of studs used in tested mock-up (147 × 50 × 1.5 mm C sections). Since full-panel approach was chosen for shear wall modelling, truss model was preferred to beam column element for intermediate studs in order to reduce the computational complexity. For intermediate studs, capacity was not limited, and brittle failure mechanisms were not modelled. The end nodes of the intermediate studs were linked by infinite rigid truss elements and they were constrained by *rigidDiaphragm* to reproduce the rigid behaviour of the floor, since the floors behaved rigidly during experiments, according to ASCE 7-10 [31].

3.2. Other components

Apart from shear walls, which represent the main lateral resisting system, there are several other components which contribute to building response, and their modelling approach is explained in this Section. Fig. 7 shows schematic drawings, representative of constructional components belonging to the first level of the mock-up.

The behaviour of gravity walls and partition walls (Fig. 7c) was also idealized as a pair of diagonal truss elements with *Pinching4* material [29]. In particular, gravity walls were calibrated on the basis of test data available for shear walls without (from test B-2650) and with (from test C-2650) finishing elements for models of Configurations B and C, respectively; whereas, since partition walls did not have finishing elements in both Configurations B and C, therefore only test data of the B-2650 shear wall were used to calibrate the *Pinching4* material.

Table 4

Cyclic parameters used in models B-2650 and C-2650.

Cyclic parameters	uForce	0
	rDisp	0.5
	rForce	0.1
Strength degradation parameters	gF,1,2	0
	gF,3,4	0
	gF, Lim	0
Unloading stiffness degradation parameters	gK,1,2	1.2
	gK,3,4	1.2
	gK, Lim	0.9
Reloading stiffness degradation parameters	gD,1,2	0.2
	gD,3,4	1.2
	gD, Lim	0.4
Energy dissipation	gE	10
Type of damage	dmgType	energy

Partition wall modelling followed the same approach employed in Leng et al. [7]. The main difference between gravity and partition walls and shear walls is represented by the *zeroLength* elements used as external constraints: hold-downs were modelled if present, in the other corners *zeroLength* elements were defined with the same properties of hold-down, but with a halved value of the tension stiffness (17.5 kN/mm). For the intermediate studs of gravity and partition walls (Fig. 7d) the same assumptions made for the shear walls were adopted.

Where the internal counter walls (Fig. 7e) were considered in the models, the studs (non-structural elements) were modelled by truss elements with physical and mechanical properties representative of profiles used in tested mock-up ($60 \times 27 \times 0.6$ mm C sections). Studs of internal counter walls were placed at a centre-to-centre distance of 98.5 mm from studs of shear or gravity walls. The end nodes of non-structural studs were linked by infinite rigid truss elements and they were constrained by the same *rigidDiaphragm* used to reproduce the rigid behaviour of the floor.

Second floor and roof were modelled following two different approaches. In the first approach, Model F1 (Fig. 8a), the diaphragm was simulated by infinite rigid vertical and horizontal beam column elements and in-plane X trusses applied at both floor lower and upper parts. The *rigidDiaphragm* constraint was applied at all joints of the floor to simulate the rigid diaphragm behaviour. In the second approach, Model F2 (Fig. 8b), the X trusses applied at floor lower part was replaced by joist elements. Joists were modelled as elastic beam column elements pin connected to the floor track elements, with the same properties of joists used in the mock-up ($197 \times 50 \times 10 \times 2.0$ mm C back-to-back section). The end nodes of joists were constrained by the same *rigidDiaphragm* used to reproduce the rigid behaviour of the floor.

The assumption of rigid diaphragm behaviour adopted in both proposed approaches is supported by experimental results, which showed that floors flexibility was low, and diaphragm behaved rigidly in its plane according to ASCE 7 [31], with a ratio between maximum diaphragm deflection and average drift of vertical element always not greater than 0.136.

3.3. Three-dimensional building

Two classes of models were developed: B models, which simulate the dynamic characteristics of mock-up in Configuration B; C models, which represent dynamic characteristics and seismic response of the building in Configuration C. Models were developed with an increasing degree of detail, ranging from using a simple pair of diagonal trusses for simulating lateral stiffness of mock-up, e.g. only shear wall without intermediate studs and finishing materials, to the use of more elements representing also other minor lateral stiffness contributing components of the mock-up, e.g. shear, gravity internal counter walls with intermediate studs and finishing materials. In particular, five different models

(B1, B2, B3, B4 and B5) were developed for the Configuration B, including shear and gravity walls without finishing non-structural elements, partition walls and floors, whereas for Configuration C six models (C1, C2, C3, C4, C5 and C6) were implemented, considering shear and gravity walls with finishing part, partition walls, floors and internal counter walls. Detailed modelling is explored and discussed, focusing the attention on main components and how they contribute to the dynamic behaviour of the mock-up. A summary is given in Table 5 to better understand all the modelling combinations.

In all the Models B1 to B5 and C1 to C6 the different structural and non-structural components already introduced were combined. For the connection among studs and floors, chord studs were linked by *zeroLength* elements, simulating hold-downs, to the bottom floor and they were rigidly connected to upper floor, whereas the ends of other studs (intermediate studs of shear walls, gravity walls and partition walls, and studs of internal counter walls) were rigidly connected to the relevant floors. Fig. 9 shows a schematic view of the C6 model, in which all the components, i.e. shear walls (with finishing and intermediate studs), floors (F2 model), gravity walls (with finishing), partition walls and internal counter walls, and their connections are represented.

Where the F1 model was used for modelling the floors, the floor seismic mass was assigned as lumped mass in the centre of the floor, whereas in the case of the F2 model the floor seismic mass was applied in the four corner points of the floor. Table 6 lists the masses applied in both types of models.

The choice of Rayleigh damping ratio value was made based on experimental results [17]. The measured damping ratio was in the range from 1% to 3% for tests carried out on the Configuration B mock-up (dynamic identification performed only before earthquake tests); from 1% to 2% for tests carried out on the Configuration C mock-up before earthquake tests; and from 2% to 5% for tests carried out on the Configuration C mock-up after earthquake tests. Since the damping choice was experimentally based, relationship between damping ratio and energy dissipation capacity was not explicitly explored. A parametric analysis was conducted to define the value of Rayleigh damping ratio, which was set equal to 4, as described in Section 5.2.

A further discussion on modelling choices employed is provided, by comparing the full-panel approach used in this study with the sub-panel approach proposed Leng et al. [7]. In particular, Table 7 provides a comparison between the modelling choices assumed by Leng et al. [7] in the Model A2d-3D-RD-a and those proposed in this paper in the Model C6. Note that models selected for the comparison are those which gave the best agreement with the experimental results.

The main differences between the two models, due also to the differences in the tested buildings, are essentially represented by the approach used for walls and diaphragms (sub-panel or full-panel approach), intermediate and chord studs modelling and hold-downs modelling.

The sub-panel approach was employed satisfactorily by Leng et al. [7,13] for shear walls, gravity walls and diaphragms in the most advanced model of CFS-NEES archetype, i.e. Model A2d-3D-RD-a. Since this approach allows to consider all main framing elements, e.g. intermediate studs and opening headers, it is capable to capture the lateral response if openings are present in the building, especially in the direction of the application of horizontal load. In fact, in case of openings, experimental results [18] showed a 3D building response with a complex load pattern which involved a not negligible of coupling among single (segment) shear walls.

The building modelled in this study does not present openings in the direction of the application of horizontal load, and some openings are located only in the walls in the direction perpendicular to the loading. This geometry is a good example in which the openings do not affect the lateral response and the load pattern can be captured by considering independent shear walls and thus with a full-panel approach.

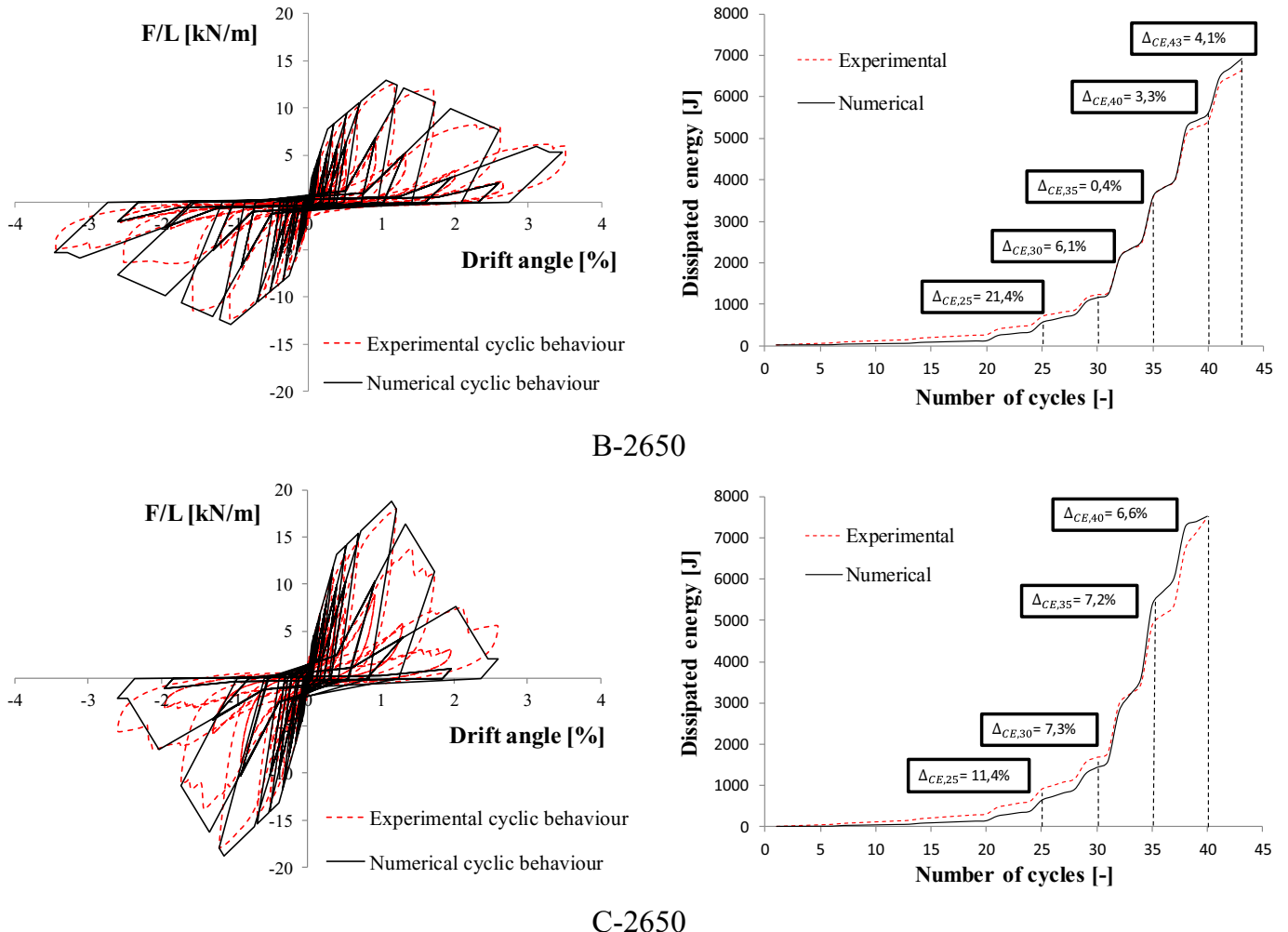


Fig. 6. Comparison between experimental and numerical cyclic response.

The modelling assumption for studs in both compared models are justified by the choice between sub-panel approach and full-panel approach. In fact, when a panel is subdivided into small parts and these small parts are modelled with diagonal trusses connected to the framing members, the best option is to model framing members through beam column elements, also accounting for the flexural behaviour. This modelling approach is well suited to include brittle failure modes of all modelled studs because the load pattern is well captured.

On the other hand, in a full-panel approach, the interaction between panel and framing members is extremely simplified and truss elements can be adopted for modelling of studs. In this case, the in plane lateral response of a shear wall is affected only by the behaviour of its chord studs, whereas intermediate studs can affect only the global behaviour of the building in terms of stiffness. Within this modelling approach, the inclusion of brittle failure modes only for chord studs can be reasonable in order to capture main possible brittle collapse under horizontal loads.

Furthermore, the hold-down modelling also differs between the two compared modelling approaches. In fact, Leng et al. [7] represented hold-downs with two nonlinear axial parallel springs, which used *Pinching4* and *ElasticPerfectlyPlastic-Gap uniaxial* materials for the tension and compression branch, respectively. The use of two parallel springs instead of one, is due to the convergence problems in case of

highly unsymmetrical nonlinear response. In C6 Model proposed, hold-downs were modelled through one spring, which used *uniaxialMaterial MinMax* in conjunction with *uniaxialMaterial ElasticMultiLinear* to explicitly model the different behaviour in tension and compression and the tensile failure. This choice was followed to keep the modelling quite light from computational point of view, but still accurate.

4. Numerical vs experimental results

Validation of numerical models was done via comparison with shake-table testing results, in term of fundamental vibration period, inter-storey drift peaks and time history. A brief overview on shake-table test results is given.

Dynamic identification test results showed that the fundamental period for the Configuration B was 0.13 s and it was greater than the period for the Configuration C before earthquake test, which was 0.10 s. Note that the variation of fundamental period was not only due to the variation of lateral stiffness, but was affected also by the variation of the mass (seismic mass of 4.04 and 8.23 t for Configurations B and C, respectively). Therefore, the fundamental period for the Configuration C was about 0.8 what it was recorded for the Configuration B, which corresponds to an increase of the stiffness of about 3 times.

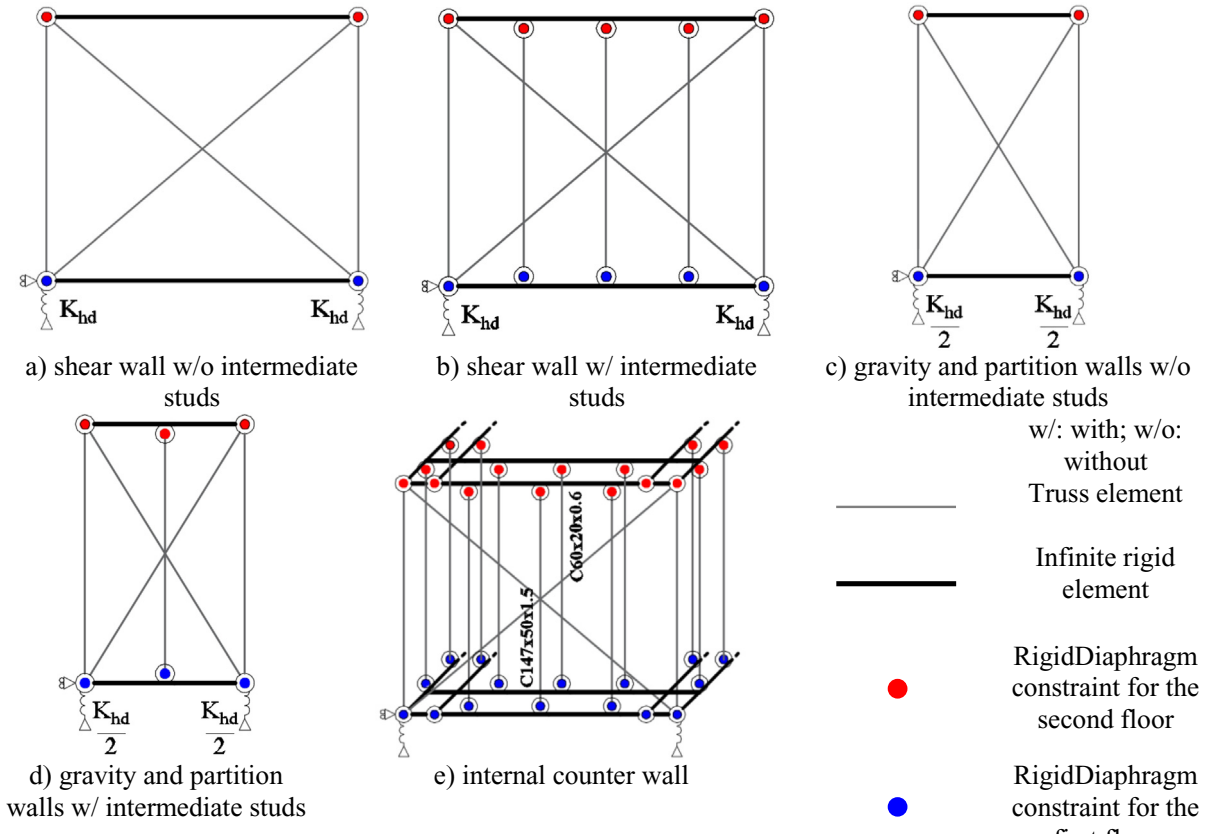


Fig. 7. Schematic drawings of modelling used for single wall components belonging to the first level.

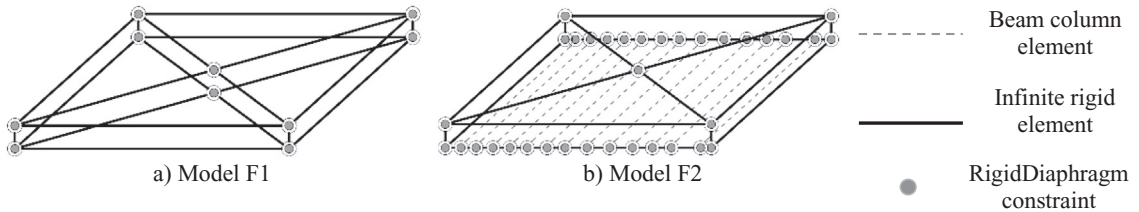


Fig. 8. Schematic drawings of modelling used for second floor and roof.

Table 5
Components in developed models.

Model	Shear walls (1)	Gravity walls (1)	Partition walls	Floors Model	Internal counter walls
B1	w/o intermediate studs	No	No	F1	No
B2	w/ intermediate studs	No	No	F1	No
B3	w/ intermediate studs	Yes	No	F1	No
B4	w/ intermediate studs	Yes	No	F2	No
B5	w/ intermediate studs	Yes	Yes	F2	No
C1	w/o intermediate studs	No	No	F1	No
C2	w/ intermediate studs	No	No	F1	No
C3	w/ intermediate studs	Yes	No	F1	No
C4	w/ intermediate studs	Yes	No	F2	No
C5	w/ intermediate studs	Yes	Yes	F2	No
C6	w/ intermediate studs	Yes	Yes	F2	Yes

(1) Shear walls and gravity walls with finishing for Models B1 to B5 and without finishing for Models C1 to C6

The increasing in stiffness because of architectural non-structural components on the single shear wall can be estimated equal to about 1.4 by comparing the lateral response of walls B-2650 and C-2650 (Figs. 5 and 6). This result confirms the important role of box building

behaviour, which increase the lateral stiffness together with the presence of architectural non-structural components.

As concerned the inter-storey drift peaks measured during earthquake tests, the positive inter-storey drift peaks were 0.80% for 1st

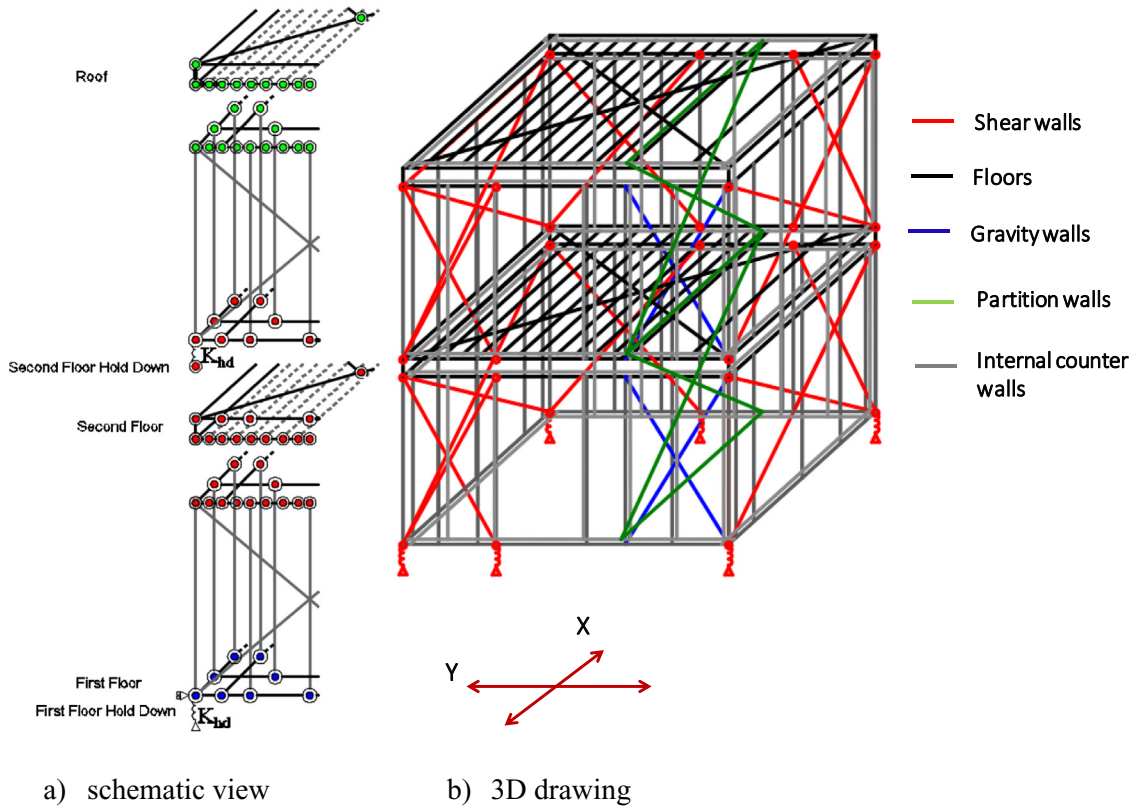


Fig. 9. Schematic view and 3D drawing of C6 model

Table 6
Masses used in models.

Floor	Masses B models [tons]	Masses C models [tons]
Second	2.54	5.19
Roof	1.50	3.04

level and 0.52% for 2nd level, whereas the negative inter-storey drift peaks were 0.35% for 1st level and 0.17% for 2nd level. All the peaks corresponded to the earthquake with maximum intensity (scale factor equal to 150%). In addition, the residual inter-story drifts were very small (under 0.05%) and the observed damage was limited to architectural non-structural components, i.e. presence of gypsum dust and small detachment of cover paper at some corner joints on the inner faces of internal counter walls.

More details about shake-table test results are available in Fiorino et al. [17].

4.1. Comparison of fundamental periods

For each model the fundamental period of vibration has been evaluated by modal analysis (T_M) and results obtained for all models are given in Table 8. In general, numerical results in terms of fundamental period capture the experimental behaviour, with fundamental periods of B Models greater than fundamental period of C Models, except for the Models B1 and C1, for which T_M is equal to 0.143 s and 0.150 s for B1 and C1 Model, respectively. This apparent paradox can be explained because when models includes only shear walls, the effect of the increasing of the mass dominates on the effect of the increasing of the stiffness.

The effect of different components on the variation of the fundamental period has been evaluated through the ratio $\Delta T_M = (T_{M,i+1} - T_{M,i})/T_{M,i}$, where $T_{M,i}$ is the fundamental period of the i^{th} Model. Components which significantly affect the numerical response in terms of fundamental period are intermediate structural studs for both B and C Models, gravity walls for C Models, partition walls for B Models.

The effect of intermediate structural studs and gravity walls on the fundamental period ($\Delta T_M = 17\%$ in B2 Model and $\Delta T_M = 36\%$ in C2 Model for intermediate structural studs, and $\Delta T_M = 17\%$ in C3 Model for gravity walls) can be explained by the increasing of the axial stiffness of walls parallel to the Y direction (perpendicular to the direction of shake-table inputs), which makes globally stiffer the structure, by emphasizing the importance of the box-building behaviour.

The partition walls were parallel to the X direction (direction of shake-table inputs) did not have finishing elements in both Configurations B and C, therefore they acted likewise to shear walls without finishing materials (the main difference between partition and shear walls without finishing materials is represented by the tension stiffness of zeroLength elements, i.e. tension stiffness of partition walls is a halved value of the tension stiffness of shear walls). As a result, partition walls decrease appreciably the fundamental period only for B Models ($\Delta T_M = 17\%$ in B5 Model), because their lateral stiffness impacts noticeably on the global lateral stiffness in B Models only.

On the other end, gravity walls in B Models, partition walls in C Models, internal-counter walls in C Models and the different modelling approaches adopted for floors does not affect significantly the numerical response in terms of fundamental period. In particular, the effect of the gravity walls in B Models is negligible ($\Delta T_M = 5\%$ in B3 Model) due to their relative low axial stiffness, caused by the lack of finishing materials. The partition walls presence (without finishing materials) slightly

Table 7

Comparison between modelling choices.

Component	Modelling approach	
	Leng et al. [7,13] – Sub-panel approach	Author proposal – Full-panel approach
Shear walls	Sub-panel model with diagonal truss elements modelled through Pinching4 material experimentally calibrated	Full-panel model with diagonal truss elements modelled through Pinching4 material experimentally calibrated
	Intermediate studs modelled as beam column elements with nominal strength capacity. Brittle failures considered	Intermediate studs modelled as elastic truss elements with nominal properties
	Chord studs modelled as beam column elements with nominal strength capacity. Brittle failures considered	Chord studs modelled as truss elements with nominal strength capacity. Brittle failures considered
	Sub-panel model with diagonal truss elements modelled through Pinching4 material experimentally calibrated	Full-panel model with diagonal truss elements modelled through Pinching4 material experimentally calibrated
	Studs modelled as beam column elements with nominal strength capacity. Brittle failures considered	Studs modelled as elastic truss elements with nominal properties
	Two parallel springs. One spring modelled with Pinching4 material. One spring modelled with Elastic Perfectly Plastic material.	Single nonlinear spring modelled with <i>uniaxialMaterial MinMax</i> in conjunction with <i>uniaxialMaterial ElasticMultiLinear</i>
Diaphragm	Semirigid diaphragm. Sub-panel model with diagonal truss elements modelled through Pinching4 material experimentally calibrated. Joists modelled as elastic beam column elements	Rigid diaphragm. Full-panel model with diagonal truss elements used in the plane of sheathing. Joists modelled as elastic beam column elements
Partition walls	Full-panel model with diagonal truss elements modelled through Pinching4 material experimentally calibrated	Full-panel model with diagonal truss elements modelled through Pinching4 material experimentally calibrated
Other non-structural components	Type: Interior gypsum sheathing.	Type: Internal counter walls and external ventilated façade.
	Modelled as additional diagonal truss elements with Pinching4 material experimentally calibrated	Modelled by changing Pinching4 material experimentally calibrated and adding non-structural studs and tracks modelled as elastic truss elements with nominal properties

decreases the fundamental period in C Models ($\Delta T_M = 6\%$ in C5 Model), because their lateral stiffness is much less than the stiffness of shear walls with finishing materials. For the C Model only, internal counter walls were added as last step. Although their presence increases the box-building behaviour, this contribution does not affect significantly the fundamental period ($\Delta T_M = 7\%$ in C6 Model) because non-structural studs and tracks adding occurs in a system already characterised by a high lateral stiffness. In the end, the different modelling approaches adopted for floors do not alter the fundamental period ($\Delta T_M = 1\%$ for both B4 and C4 Models) because joists do not play any role in the transfer of horizontal forces.

Fundamental period of vibrations evaluated by modal analysis (T_M) have been compared with those evaluated during the experimental tests (T_E) through the ratio $\Delta T_{ME} = (T_M - T_E)/T_E$ (Table 8). ΔT_{ME} is in

Table 8

Comparison between experimental and numerical results in term of fundamental period of vibration.

Model	Features (1)	T_E [s]	T_M [s]	ΔT_M [%]	T_D [s]	ΔT_{ME} [%]	ΔT_{DE} [%]
B1	Shear walls w/o intermediate studs, Floors Model F1	0.126	0.143	–	–	13	–
B2	As B1, but shear walls w/ intermediate studs		0.123	17	0.123	-2	-2
B3	As B2, plus Gravity walls	0.118	5	–	–	-6	–
B4	As B3, but Floors Model F2	0.117	1	–	–	-7	–
B5	As B4, plus Partition walls	0.100	17	0.110	-21	-13	–
C1	Shear walls w/o intermediate studs, Floors Model F1	0.102	0.150	–	–	47	–
C2	As C1, but shear walls w/ intermediate studs	0.111	36	–	9	–	–
C3	As C2, plus Gravity walls	0.095	17	0.100	-7	-2	–
C4	As C3, but Floors Model F2	0.093	1	–	–	-9	–
C5	As C4, plus Partition walls	0.088	6	–	–	-14	–
C6	As C5, plus internal counter walls	0.082	7	0.091	-20	-11	–

(1) Shear walls and gravity walls without finishing for Models B1 to B6 and with finishing for Models C1 to C7

the range from -21% to 13% for B Models and from -20 to 47% for C Models. In particular, models with only shear walls overestimate the experimental fundamental period of vibrations (13% and 47% for B1 and C1 Models, respectively) and models with all components underestimate the experimental fundamental period of vibrations (-21% and -20% for B5 and C6 Models, respectively). The most accurate predictions of experimental fundamental period of vibration are obtained through the model with shear walls including intermediate structural studs and Model F1 for floors for Configuration B (B2 Model, $\Delta T_{ME} = -2\%$) and model with shear walls including intermediate structural studs, gravity walls and Model F1 for floors for Configuration C (C3 Model, $\Delta T_{ME} = -7\%$).

Since the structural system under investigation is characterised by a nonlinear lateral response also for small horizontal actions, also the modality used to evaluate the fundamental vibration period can affect the results. For this reason, fundamental vibration periods have also been evaluated on the bases of time history analysis performed by means of numerical models under the same white noise inputs used during the RND experimental tests (T_D). In particular, the same procedure used for the experimental dynamic identification has been applied to the results obtained with the time history analyses, i.e. the fundamental vibration frequencies have been calculated as the first peak of the frequency response function (transfer function) in the frequency domain, obtained as the ratio between the Fourier transformation of the input acceleration and the roof accelerations obtained by time history analysis.

Only B2, B5, C3 and C6 Models have been considered for this purpose. In particular, T_D evaluated according this procedure is equal to 0.123 s and 0.110 s for B2 and B5 Models, respectively, and 0.100 s and 0.091 s for C3 and C6 Models, respectively. Results show that fundamental periods evaluated by time history analysis are equal to or slightly higher (within 11%) than those obtained by modal analysis. In addition, the differences between time history analysis and modal analysis increase when the models include multiple components. This is reasonable because the softening related to nonlinear behaviour corresponds to a reduction of lateral stiffness and this occurrence increases as nonlinear sources, i.e. the number of components, increase. The ratio T_E has been used to compare fundamental vibration periods obtained by numerical time history analysis and experimental results. The ratio ΔT_{DE} is equal to -2% and -13% for B2 and B5 Models, respectively, and it is equal to -2% and -11% for C3 and C6 Models, respectively. In conclusion, the estimation of fundamental vibration period evaluated by time history analysis is more than acceptable, offering very good

previsions, which are better than previsions given by modal analysis, especially for C Models.

4.2. Comparison of inter-storey drifts

The developed models were subjected to nonlinear time history analysis under the earthquake input to investigate their seismic behaviour. Numerical results are discussed for the simplest C1 Model; for the C3 Model, which gives the best prediction of first period of vibration; and for the most advanced C6 Model. As already introduced, in the experimental activity the mock-up was subjected to sequences of earthquakes with different scaling factors (Table 1). To make more comparable experimental and numerical results the same earthquake input sequences were implemented in OpenSees for earthquake analysis. More details about the earthquake sequence effect are given in Section 5.1. The inputs used in numerical analysis were the accelerations measured at the mock-up base (actual input), instead of the original earthquake record (target input).

Numerical and experimental time histories in terms of inter-storey drift ratio (IDR) are compared for the input having the higher scaling factor (EA_4_17) in Figs. 10 and 11. It is clear that the C6 Model gives the best prediction, while C1 Model and C3 Model overestimate the IDRs.

A quantitative comparison between numerical and experimental results obtained for the input EA_4_17 is presented in terms of peak inter-storey drift ratio (PIDR) in Table 9 through the ratio $\Delta_{NE} = (\text{PIDR}_N - \text{PIDR}_E) / \text{PIDR}_E$, where PIDR_N and PIDR_E are the numerical and experimental PIDRs, respectively. Results show that C1 Model significantly overestimates the seismic response of the mock-up, with a ratio Δ_{NE} of 81% and 64% for first and second storey, respectively. Although C3 Model gives the best prediction of the first period of vibration, PIDRs are slightly over-estimated and the ratio Δ_{NE} is equal to 14% and 53% for first and second storey, respectively. The C6 Model, which takes into account of all structural and architectural non-structural components gives the better estimation of PIDRs, with a ratio Δ_{NE} of -24% and 2% for first and second storey, respectively. These results show the big role of architectural non-structural components, especially when the building is subjected to high intensity earthquakes. This statement could be also confirmed by the comparison between numerical results for C3 and C6 Models (C1 Model is completely inadequate to represent both dynamic and seismic behaviour of mock-up) and experimental PIDRs evaluated for low-intensity earthquakes, e.g., earthquakes with scaling factor equal to 50%. As a matter of fact, for the input EA_4_10 the PIDR is more accurately predicted by C3 Model, with a Δ_{NE} equal to 26% and 39% for first and second storey, respectively, while C6 Model largely underestimates the PIDR, with a Δ_{NE} equal to about 75% and 66% for first and second storey, respectively, as summarized in Table 10.

5. Effect of earthquake sequence and damping

In this Section a further discussion of results is presented. In particular, it is shown how the application of earthquake inputs in sequence or separately (earthquake sequence effect) and the choice of different damping ratio values (damping value effect) affect results. For this scope, C6 Model was chosen because it gives the most accurate prediction of the mock-up seismic response, as discussed before.

5.1. Earthquake sequence effect

Figs. 12 and 13 compare numerical and experimental first storey IDR time histories for the input having the higher scaling factor (EA_4_17), where numerical time-history considers input sequence or not. In particular, where numerical time-history takes in to account the input sequence all earthquake inputs from EA_2_01 to EA_4_17 have been adopted (Numerical results C6), whereas the numerical analysis under the single input EA_4_17 has been carried out as comparison (Numerical result C6_no sequence). Figs. 12 and 13 show that if the analysis does not account for the earthquake sequence effect the IDR can be significantly underestimated. In particular, for the selected case, when the input EA_4_17 is applied without sequence effect Δ_{NE} is 45% and 55% for first and second storey, respectively (PIDR_E of 0.80% and 0.52% and PIDR_N of 0.43% and 0.20% for first and second storey, respectively), whereas, when the same input is applied by considering the sequence effect the same results shown in Section 4.2 is obtained (Δ_{NE} is 24% and 2% for first and second storey, respectively, see Table 9).

5.2. Damping

The choice of damping ratio has an enormous importance for the numerical response under earthquake excitations in CFS sheathing-braced structures. In order to validate the damping ratio equal to 4% adopted in the presented study, a comparison in term of IDR time-history obtained with different values of damping ratio has been carried out. In particular, damping ratios equal to 2%, adopted by Shamim and Rogers [22], and 5%, used in Leng et al. [7], were adopted for the comparison.

Fig. 14 shows the IDR numerical time histories obtained with the C6 Model by using damping ratios of 2%, 4% and 5% compared with the experimental result. Inputs were applied taking it to account of earthquake sequence for all numerical analyses.

From comparison between experimental and numerical results, three different ranges during the time history can be noticed. In the first range (for time less than about 6.5 s), which is characterised by reaching the PIDR, the best fit response between numerical and experimental results is obtained for a damping ratio equal to 2% (2% best-fit zone in Fig. 14). In the second range (for time from about 6.5 s to about 14 s), which is characterised by a small reduction of IDRs, the best fit is reached for a damping ratio of 4% (4% best-fit zone in Fig. 14). In the third range (for time more than about 14 s), which is

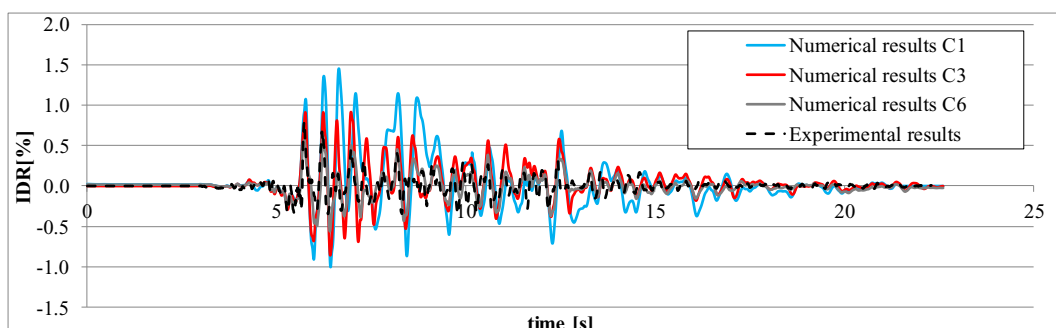


Fig. 10. Experimental and Numerical inter-storey drift (IDR) time history for first storey.

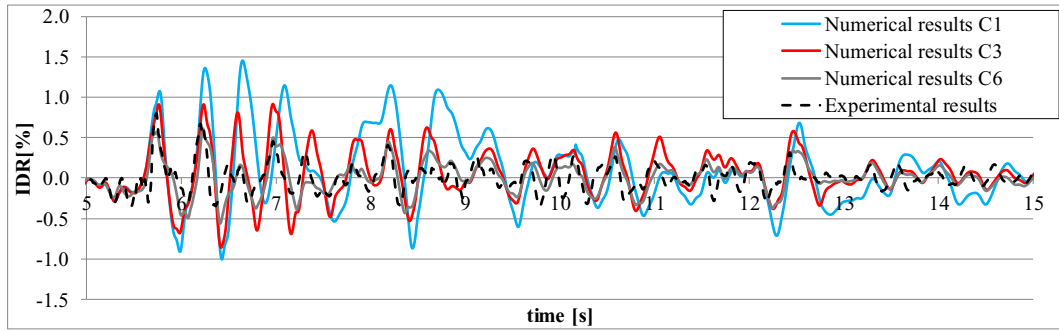


Fig. 11. Extract of inter-storey drift (IDR) time history recorded between 5 and 15 s.

Table 9

Comparison between experimental and numerical PIDR for the input EA_4_17 (scaling factor 150%).

Storey	Model	PIDR _N [%]	PIDR _E [%]	Δ_{NE} [%]
1	C1	1.45	0.80	81
	C3	0.91		14
	C6	0.61		-24
2	C1	0.85	0.52	64
	C3	0.79		53
	C6	0.53		2

Table 10

Comparison between experimental and numerical PIDR for the input EA_4_10 (scaling factor 50%).

Storey	Model	PIDR _N [%]	PIDR _E [%]	Δ_{NE} [%]
1	C3	0.18	0.24	26%
	C6	0.06		75%
2	C3	0.15	0.13	39%
	C6	0.08		66%

characterised by a significant reduction of IDRs, the best fit is obtained for a damping ratio equal to 5% (5% best-fit zone in Fig. 14). However, the difference between results obtained with damping ratios equal to 4% and 5% is not significant and both assumptions underestimate the IDRs for a time less than about 6.5 s, whereas they describe the response with enough accuracy for a time more than about 6.5 s.

Therefore, in order to have a better agreement between numerical and experimental response a model with variable damping ratio should be the best choice, in which lower values should be set when the building experiences higher IDRs and higher values should be adopted when

IDRs decrease. This circumstance could be explained by the fact that some sources of damping are not well described by the cyclic model and they become significant when the plastic engagement of the structure decreases.

6. Conclusions

The paper presents the modelling of a full-scale two-storey CFS building, subjected to shake-table tests, carried out at University of Naples Federico II, as a part of the ELISSA project. Shake-table tests were performed to investigate on seismic behaviour of CFS buildings. The case-study mock-up was built in two different stages: in the first phase, named as bare structure (Configuration B), the mock-up was mainly composed of shear walls and gravity walls without finishing parts, internal partition walls, floors and roof; in the second configuration, named as complete construction (Configuration C), all non-structural components, such as internal counter walls and finishing parts of shear walls, gravity walls, and finishing parts of floors and roof, were added. Two different types of input signals were chosen: white noise and earthquake signals. White noise inputs were applied to both Configurations B and C for the dynamic identification, while earthquake inputs were applied only to the Configuration C for the evaluation of seismic response.

Then, the numerical modelling of the mock-up was developed through the OpenSees software. Firstly, main lateral resisting system, i.e. shear walls, were modelled as a pair of diagonal truss elements, calibrated on the base of experimental data. Subsequently, five models for Configuration B mock-up (B Models), including shear and gravity walls without finishing non-structural elements, partition walls and floors, and six models for Configuration C mock-up (C Models), considering shear and gravity walls with finishing part, partition walls, floors and internal counter walls, were developed.

Comparing the experimental and numerical fundamental periods, it was clear that the models in which only shear walls are explicitly

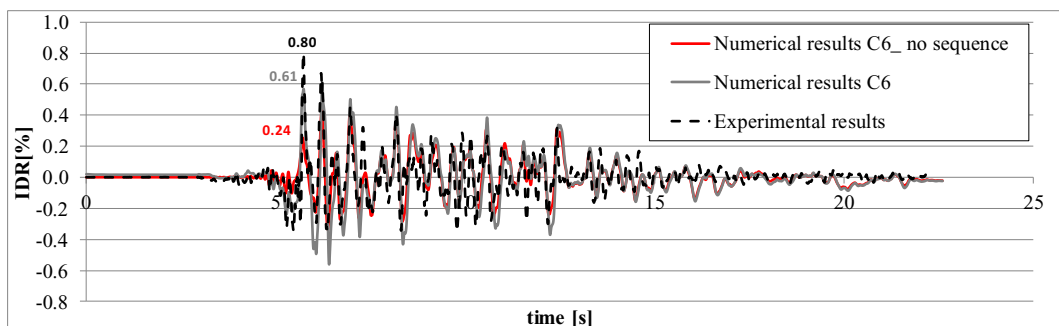


Fig. 12. Sequence effect on numerical IDR time history for first storey.

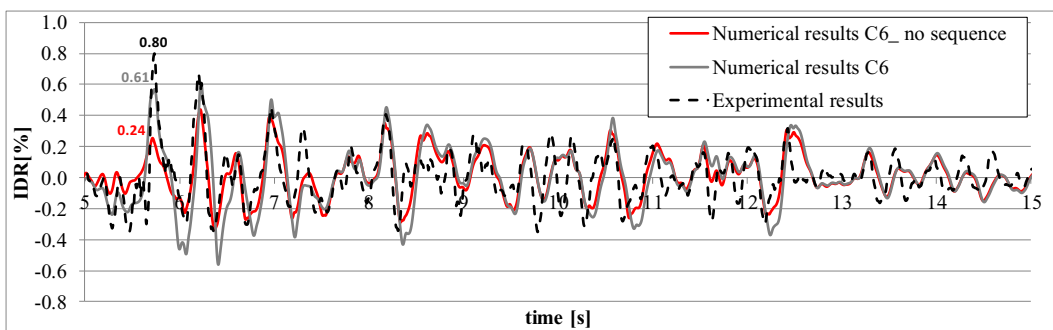


Fig. 13. Extract of sequence effect on numerical IDR time history recorded between 5 and 15 s.

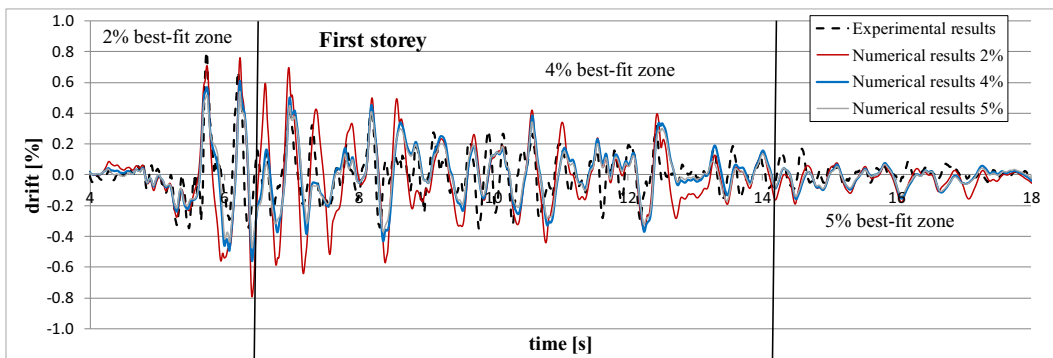


Fig. 14. Damping value effect on IDR time history for first storey considering damping ratio equal to 2%, 4% and 5%.

considered are unsuitable to represent the dynamic behaviour of mock-up in both Configurations B and C. The models which best predict the dynamic response of mock-up for the Configuration B are the models in which shear walls and intermediate studs were explicitly modelled, whereas for the Configuration C the best prediction is given by the models in which shear walls, intermediate studs and gravity walls are explicitly modelled.

The comparison between experimental and numerical results in terms of inter-storey drift peaks and time history under earthquake inputs shows that the best prediction is given by the most advanced model, in which all the structural and non-structural components are explicitly considered. In fact, it accurately catches the peak inter-storey drifts under the input having the maximum intensity, with an error of 24% and 2% for first and second storey, respectively.

In addition, from the comparison between experimental and numerical inter-storey drift time history, it was found that, if the numerical analysis does not account for the earthquake sequence effect, the inter-storey drift peaks are significantly underestimated of about 45% and 55% for first and second storey, respectively.

Finally, the results show that the damping increased as the damage progressed and the best fit between experimental and numerical behaviour would be obtained if an increasing damping ratio from 2% to 5% is adopted during the time history. However, the assumption of a constant damping ratio of 4% simulates with satisfactory level of accuracy the seismic response over the complete time history and represents a good compromise between accuracy and easy modelling.

In conclusion, the most advanced model proposed in this paper, which considers all the structural and non-structural components and a damping ratio of 4%, simulates with good accuracy the seismic response of the mock-up if the input sequence is accounted. Indeed, full-panel approach works well in ELISSA mock-up modelling, capturing the seismic response and saving computational cost, but this is a specific

result which cannot be generalized for all CFS sheathed buildings, especially for building characterised by many openings, in which complex load pattern involving a not negligible coupling among single (segment) shear walls can affect the lateral response.

Acknowledgements

The study presented in this paper is a part of the project "Energy Efficient Lightweight-Sustainable-SAfe-Steel Construction" (Project acronym: ELISSA) coordinated by Prof. Raffaele Landolfo for the research activities of the University of Naples "Federico II". The project has received funding from the European Union Seventh Framework Programme (FP7/2007-2013) under grant agreement n609086.

Author statement

Numerical modelling of CFS two-storey sheathing-braced building under shaking-table excitations.

Declaration of Competing Interest

The authors declare that they have no known competing financial interests or personal relationships that could have appeared to influence the work reported in this paper.

References

- [1] J. Goggins, S. Salawdeh, Validation of nonlinear time history analysis models for single-storey concentrically braced frames using full-scale shake table tests, *Earthq. Eng. Struct. Dyn.* 42 (2013) 1151–1170, <https://doi.org/10.1002/eqe.2264>.
- [2] Y. Chen, W. Wang, Y. Chen, Full-scale shake table tests of the tension-only concentrically braced steel beam-through frame, *J. Constr. Steel Res.* 148 (2018) 611–626, <https://doi.org/10.1016/j.jcsr.2018.06.017>.

- [3] A.A. Rad, G.A. MacRae, N.K. Hazaveh, Q. Ma, Shake table testing of a low damage steel building with asymmetric friction connections (AFC), *J. Constr. Steel Res.* 155 (2019) 129–143, <https://doi.org/10.1016/j.jcsr.2018.12.013>.
- [4] A. Hammad, M.A. Moustafa, Shake table tests of special concentric braced frames under short and long duration earthquakes, *Eng. Struct.* 200 (2019) 109695, <https://doi.org/10.1016/j.engstruct.2019.109695>.
- [5] N. Bourahla, T. Boukhemacha, N. Allal, A. Attar, Equivalent shear link modeling and performance analysis of cold formed steel structures under earthquake loading, *Proc. 9th U.S. Natl. 10th Can. Conf. Earthq. Eng.* (2010), 1063.
- [6] J. Martínez-Martínez, L. Xu, Simplified nonlinear finite element analysis of buildings with CFS shear wall panels, *J. Constr. Steel Res.* 67 (2011) 565–575, <https://doi.org/10.1016/j.jcsr.2010.12.005>.
- [7] J. Leng, K.D. Peterman, G. Bian, S.G. Buonopane, B.W. Schafer, Modeling seismic response of a full-scale cold-formed steel-framed building, *Eng. Struct.* 153 (2017) 146–165, <https://doi.org/10.1016/j.engstruct.2017.10.008>.
- [8] L. Fiorino, S. Shakeel, V. Macillo, R. Landolfo, Seismic response of CFS shear walls sheathed with nailed gypsum panels: numerical modelling, *Thin-Walled Struct.* 122 (2018) 359–370, <https://doi.org/10.1016/j.tws.2017.10.028>.
- [9] L. Fülöp, D. Dubina, Performance of wall-stud cold-formed shear panels under monotonic and cyclic loading, *Thin-Walled Struct.* 42 (2004) 339–349, [https://doi.org/10.1016/S0263-8231\(03\)00064-8](https://doi.org/10.1016/S0263-8231(03)00064-8).
- [10] I. Shamim, C.A. Rogers, Steel sheathed/CFS framed shear walls under dynamic loading: numerical modelling and calibration, *Thin-Walled Struct.* 71 (2013) 57–71, <https://doi.org/10.1016/j.tws.2013.05.007>.
- [11] S. Kechidi, N. Bourahla, Deteriorating hysteresis model for cold-formed steel shear wall panel based on its physical and mechanical characteristics, *Thin-Walled Struct.* 98 (2016) 421–430, <https://doi.org/10.1016/j.tws.2015.09.022>.
- [12] V. Macillo, S. Shakeel, L. Fiorino, R. Landolfo, Development and calibration of a hysteretic model for CFS strap braced stud walls, *Adv. Steel Constr.* 14 (2018) <https://doi.org/10.18057/JIASC.2018.14.3.2>.
- [13] J. Leng, PhD Thesis Simulation of Cold-Formed Steel Structures., Johns Hopkins University, 2015.
- [14] K.D. Peterman, M.J.J. Stehman, R.L. Madsen, S.G. Buonopane, N. Nakata, B.W. Schafer, Experimental seismic response of a full-scale cold-formed steel-framed building. II: subsystem-level response, *J. Struct. Eng.* 142 (2016) [https://doi.org/10.1016/\(ASCE\)ST.1943-541X.000157804016128](https://doi.org/10.1016/(ASCE)ST.1943-541X.000157804016128).
- [15] B.W. Schafer, D. Ayhan, J. Leng, P. Liu, D. Padilla-Illano, K.D. Peterman, M. Stehman, S.G. Buonopane, M. Eatherton, R. Madsen, B. Manley, C.D. Moen, N. Nakata, C. Rogers, C. Yu, Seismic Response and Engineering of Cold-formed Steel Framed Buildings, 2016<https://doi.org/10.1016/j.istruc.2016.05.009>.
- [16] K.D. Peterman, M.J.J. Stehman, R.L. Madsen, S.G. Buonopane, N. Nakata, B.W. Schafer, Experimental seismic response of a full-scale cold-formed steel-framed building. I: system-level response, *J. Struct. Eng.* 142 (2016) [https://doi.org/10.1016/\(ASCE\)ST.1943-541X.000157704016127](https://doi.org/10.1016/(ASCE)ST.1943-541X.000157704016127).
- [17] L. Fiorino, V. Macillo, R. Landolfo, Shake table tests of a full-scale two-story sheathing-braced cold-formed steel building, *Eng. Struct.* 151 (2017) 633–647, <https://doi.org/10.1016/j.engstruct.2017.08.056>.
- [18] B.W. Schafer, D. Ayhan, J. Leng, P. Liu, D. Padilla-Illano, K.D. Peterman, M. Stehman, S. G. Buonopane, M. Eatherton, R. Madsen, B. Manley, C.D. Moen, N. Nakata, C. Rogers, C. Yu, Seismic response and engineering of cold-formed steel framed buildings, *Structures* 8 (2016) 197–212, <https://doi.org/10.1016/j.istruc.2016.05.009>.
- [19] M.S. Hoehler, C.M. Smith, T.C. Hutchinson, X. Wang, B.J. Meacham, P. Kamath, Behavior of steel-sheathed shear walls subjected to seismic and fire loads, *Fire Saf. J.* 91 (2017) 524–531, <https://doi.org/10.1016/j.firesaf.2017.03.021>.
- [20] I. Shamim, D. Morello, C.A. Rogers, Dynamic testing and analyses of wood sheathed/CFS framed shear walls, 9th US Natl. 10th Can. Conf. Earthq. Eng., 2010 , Toronto, Canada. p. Paper No. 1069.
- [21] I. Shamim, J. DaBreo, C.A. Rogers, Dynamic testing of single- and double-story steel-sheathed cold-formed steel-framed shear walls, *J. Struct. Eng.* 139 (2013) 807–817, [https://doi.org/10.1061/\(ASCE\)ST.1943-541X.0000594](https://doi.org/10.1061/(ASCE)ST.1943-541X.0000594).
- [22] I. Shamim, C.A. Rogers, Numerical evaluation: AISI S400 steel-sheathed CFS framed shear wall seismic design method, *Thin-Walled Struct.* 95 (2015) 48–59, <https://doi.org/10.1016/j.tws.2015.06.011>.
- [23] R. Landolfo, O. Luorio, F. Luigi, Experimental seismic performance evaluation of modular lightweight steel buildings within the ELISSA project, *Earthq. Eng. Struct. Dyn.* (2018) 1–23, <https://doi.org/10.1002/eqe.3114>.
- [24] CEN, EN 1998–1 Eurocode 8, Design of Structures for earthquake resistance-Part 1: General rules, seismic actions and rules for buildings, European Committee for Standardization, Brussels, 2004.
- [25] . CEN, EN 1993-1-3, Eurocode 3: Design of steel structures-Part 1–3: General rules-Supplementary rules for cold-formed members and sheeting, European Committee for Standardization, Brussels, 2006.
- [26] Cocoon, Transformer, ETA-11/0105, 2010.
- [27] S. Mazzoni, F. McKenna, M.H. Scott, G.L. Fenves, Open System for Earthquake Engineering (OpenSees) (2009).
- [28] V. Macillo, L. Fiorino, R. Landolfo, Seismic response of CFS shear walls sheathed with nailed gypsum panels: experimental tests, *Thin-Walled Struct.* 120 (2017) 161–171, <https://doi.org/10.1016/j.tws.2017.08.022>.
- [29] L.N. Lowes, N. Mitra, A. Alootash, A beam-column joint model for simulating the earthquake response of reinforced concrete frames a beam-column joint model for simulating the earthquake response of reinforced concrete frames, PEER report 2003/10, PEER Rep. 2004 (2003/10).
- [30] H. Kravinkler, P. Francisco, L. Ibarra, A. Ayoub, R. Medina, CUREE publication No. W-02 Development of a Testing Protocol for Woodframe Structures, 2001.
- [31] SEI/ASCE, ASCE 7–10 Minimum Design Loads for Buildings and Other Structures, American Society of Civil Engineers, Reston, Virginia, 2010.